

# A high-drop hole-type photonic crystal add-drop filter\*

JIANG Jun-zhen (蒋俊贞)<sup>1</sup>, QIANG Ze-xuan (强则焯)<sup>1\*\*</sup>, ZHANG Hao (张昊)<sup>1,2</sup>, ZHENG Yan-min (郑彦敏)<sup>1</sup>, and QIU Yi-shen (邱怡申)<sup>1</sup>

1. Fujian Provincial Key Laboratory for Photonics Technology, Key Laboratory of Optoelectronic Science and Technology for Medicine, Ministry of Education, Institute of Laser and Optoelectronics Technology, Fujian Normal University, Fuzhou 350007, China

2. Department of Electronic Information Science, Fujian Jiangxia College, Fuzhou 350007, China

(Received 30 September 2013)

©Tianjin University of Technology and Springer-Verlag Berlin Heidelberg 2014

Based on the effect of total internal reflection (TIR) and photonic band gap, a new type of hexagonal-lattice hole-type silicon photonic crystal add-drop filter is proposed with a large circular hole as inner ring. The single mode operation is realized by compressing the two rows of photonic crystal above and below the line defect waveguide. Two-dimensional (2D) finite-difference time-domain (FDTD) method is then applied to investigate the impacts of side length of inner ring and coupling strength on its drop efficiency. It is also fairly compared with the traditional inner ring structure composed of hexagonal-lattice holes. The results show that the proposed structure can offer higher spectral selectivity than the traditional one. Two channel wavelengths of 1.425  $\mu\text{m}$  and 1.45  $\mu\text{m}$  can be simultaneously dropped at corresponding ports with drop efficiency of more than 90% and quality factor of 900 in the proposed configuration when the width of bus waveguide, the side length of inner ring and the coupling strength are  $0.8\sqrt{3}a$ ,  $4a$  and 0, respectively, where  $a$  is the lattice constant.

**Document code:** A **Article ID:** 1673-1905(2014)01-0034-4

**DOI** 10.1007/s11801-014-3180-1

Optical add-drop filters (OADFs)<sup>[1-3]</sup> are essential building blocks to construct various photonic components used in optical communication, such as optical multiplexers, optical modulators and optical switches. Waveguide ring resonator based OADFs have been successfully demonstrated owing to their high spectral selectivity and wide free spectral range (FSR). However, its size is intrinsically limited by the guided mechanism of total internal reflection (TIR). On the other hand, photonic crystal ring resonators (PCRRs)<sup>[4]</sup> have attracted much interest for their high coupling efficiency, scalable ring sizes, independent transmission loss, compact overall structure and flexible mode coupling configurations<sup>[4,5]</sup>. Potentially, they present a solution to overcome the scaling obstacle of traditional ring resonators. In the past few years, PCRR-based OADFs have been experimentally and theoretically demonstrated<sup>[6-11]</sup>, and most reports were based on dielectric-rod photonic crystals. The dielectric-rod type can theoretically demonstrate the high drop efficiency. But it is practically complicated and difficult to fabricate for offering vertical confinement and reducing propagation losses<sup>[6-8]</sup>. By contrast, the hole-type PCRR is much easier to fabricate while its drop efficiency is typically low due to the exci-

tation of multimode behavior<sup>[9-11]</sup>.

It is thus very significant to develop a high-drop hole-type PCRR-based OADF. In this paper, we present a new configuration of PCRR based on a large circular hole instead of traditional hexagonal-lattice holes, which utilizes the effect of photonic band gap and TIR. The technique compressing the two rows of photonic crystal above and below the line defect waveguide is introduced to realize single mode operation. For comparison, the traditional inner ring structure composed of hexagonal-lattice holes is also investigated. The performance of two hole-type PCRR-based OADFs is numerically analyzed by using two-dimensional (2D) finite-difference time-domain (FDTD) method.

The schematic diagrams of the two proposed hexagonal-lattice PCRRs with a large circular hole and traditional hexagonal-lattice holes as inner ring are shown in Fig.1(a) and (b), respectively. The two PCRRs are both composed of 2D cylindrical air holes in silicon substrate with refractive index of  $n_{\text{Si}}=3.48$ . The thickness of silicon substrate is  $0.5a$ , and the air-hole radius  $r$  is  $0.35a$ , where  $a$  is the lattice constant. The  $W0.8$  bus waveguide with width of  $0.8\sqrt{3}a$  is formed by removing one line of air-holes along  $\Gamma K$  direction and compressing the two

\* This work has been supported by the Natural Science Foundation of Fujian Province of China (No.2012J01253).

\*\* E-mail: qiangzx@fjnu.edu.cn

rows of photonic crystal above and below the line defect waveguide. The incident port and exit ports are labeled as  $A$  and  $B$ ,  $C$ ,  $D$ , respectively. The surrounding periods of the  $W0.8$  bus waveguide and ring resonator are both 16, i.e.,  $d_1=16a$  and  $d_2=16a$ , respectively. The coupling strength, which is defined as the number of coupling periods between the bus waveguide and the PCRRs, is  $L_c=a$ . The side lengths of two types of inner rings keep the same as  $L=3a$ . The radius of large circular hole  $R_c$  shown in Fig.1(a) is  $1.5a$  according to the concept of effective ring radius. For the accurate analysis on the transmission characteristics of above configurations, three-dimensional (3D) FDTD is necessary. However, the fully vectorial 3D FDTD method extremely consumes time and computer memory. The effective index method (EIM) has proved to be very effective in predicting results with reduced dimensionality from 3D to 2D<sup>[12-14]</sup>, which is the most effective for the low index contrast structure especially. However, it becomes less accurate when it is applied to high index contrast structure, such as silicon on the insulating substrate. In the early work, our team introduced an effective index perturbation (EIP) technique<sup>[15]</sup> for determining the suitable effective index for the high index contrast structure based on 2D plane-wave expansion (PWE) techniques and 2D FDTD method. For simplicity, here we only use 2D numerical technique to analyze the performance of the designed OADF. The index of background is set as 2.7 based on EIP.

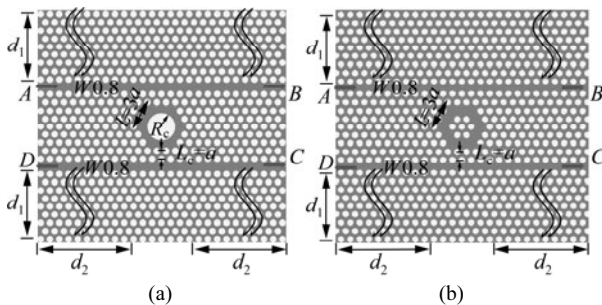


**Fig.1 Schematic diagrams of hexagonal-lattice PCRRs with (a) a large circular hole and (b) traditional hexagonal-lattice holes as the inner ring**

The simulated dispersion plots of TE polarization along  $\Gamma K$  direction are shown in Fig.2. The regular  $W1$  bus waveguide with width of  $\sqrt{3}a$  shown in Fig.2(a) will support multimode operation. When we reduce the width to  $0.8\sqrt{3}a$ , i.e.,  $W0.8$  bus waveguide, by compressing the two rows of photonic crystal above and below the line defect waveguide, there exhibits a broadband single-mode range with frequency from  $0.294a/\lambda$  to  $0.356a/\lambda$ . For the high-drop purpose, this bus width is kept as  $0.8\sqrt{3}a$  in the subsequent discussions. For the  $1.55\mu\text{m}$  communication window,  $a$  is set as  $504\text{ nm}$ .

The transmission characteristics are then simulated with a free open 2D FDTD technique using perfectly matched layer (PML) as the absorbing boundary condition. A

Gaussian TE polarization optical pulse, which covers the whole frequency range of interest, is launched at the input port  $A$ . Power monitors are placed at all of the other three ports ( $B$ ,  $C$  and  $D$ ) to detect the transmitted spectral power densities after Fourier transformation. All of the transmitted spectral power densities are normalized to the incident light spectral power density from input port  $A$ .

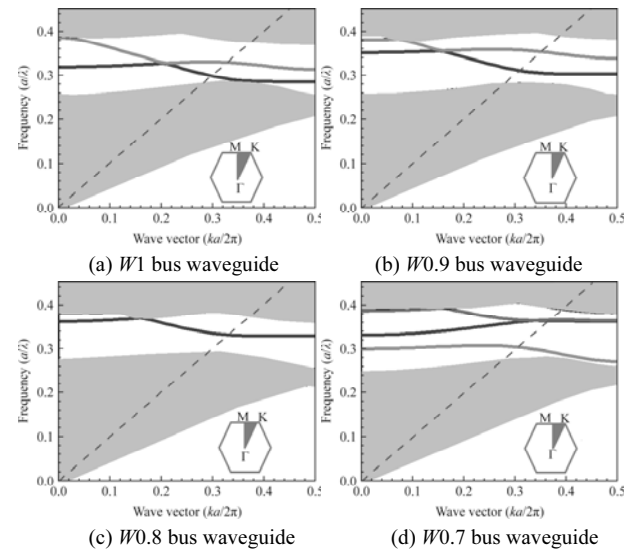
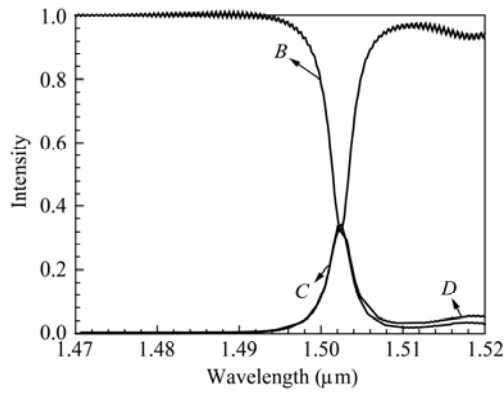


**Fig.2 Simulated dispersion results of incident TE polarization with different bus waveguides**

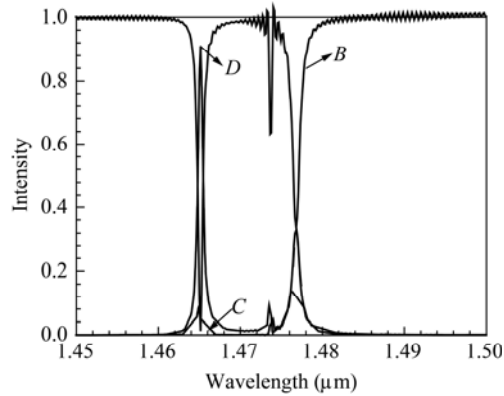
The normalized transmission intensity spectra of above two configurations at  $B$ ,  $C$  and  $D$  output ports are shown in Fig.3. Quality factor is defined as the ratio of full width at half maximum (FWHM) to the center wavelength of the dropped channel. For the PCRR with traditional hexagonal-lattice holes, drop efficiency of 34% and quality factor of 470 can be obtained at  $1.503\mu\text{m}$  signal channel at port  $D$ , while our proposed configuration with a large circular hole can offer drop efficiency of 91% and quality factor of 2100 at  $1.465\mu\text{m}$ .

We also investigate the impacts of  $L$  and  $L_c$  on the drop efficiency of both two configurations. Figs.4 and 5 show their normalized output intensities at port  $D$  with various  $L$  and  $L_c$ . The side length  $L$  ranging from  $3a$  to  $6a$  will greatly affect the drop wavelengths and efficiencies of both two configurations. It is obvious from Fig.5 that our proposed structure can always offer higher spectral selectivity and drop efficiency for  $L_c=0$  and  $a$ . For our proposed configuration, when the coupling strength is weakened, i.e.,  $L_c=0$ , the higher drop efficiency can be obtained. Besides, the smaller side length can offer the higher drop efficiency. For example, for  $L=4a$  and  $L_c=0$  shown in Fig.5(b), it can provide the drop efficiency of about 90.2% and quality factor of 1500 at  $1.45\mu\text{m}$ .

The intensity spectra of other output ports in our proposed structure are also shown in Fig.6. It is very interesting that it can also drop at  $1.425\mu\text{m}$  with drop efficiency of 92.7% and quality factor of 950.

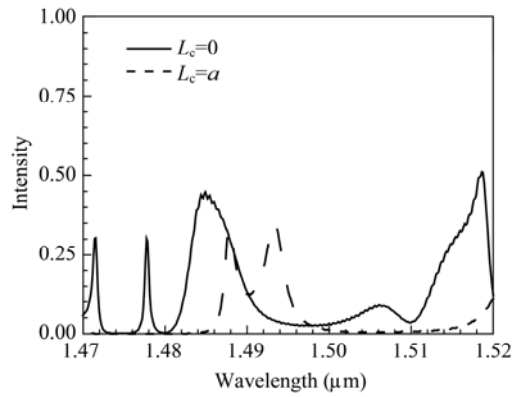


(a)

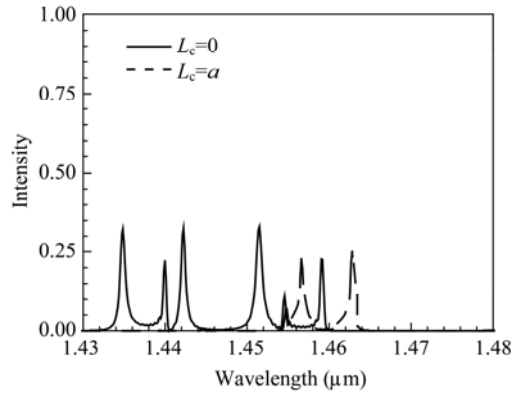


(b)

**Fig.3** Transmission spectra of TE polarization at three output ports *B*, *C* and *D* for PCRRs with (a) traditional hexagonal-lattice inner ring and (b) a large circular-hole inner ring

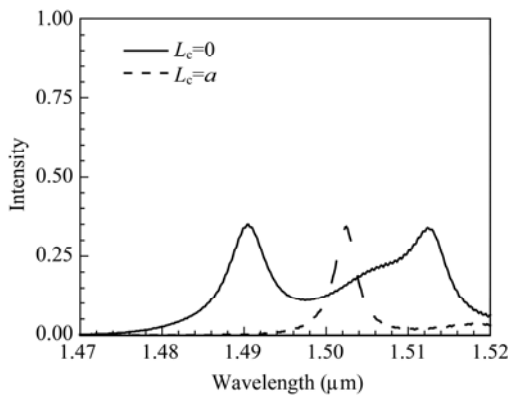


(c)  $L_c=5a$

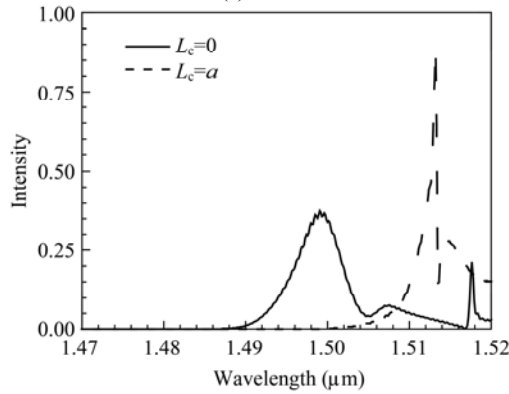


(d)  $L=6a$

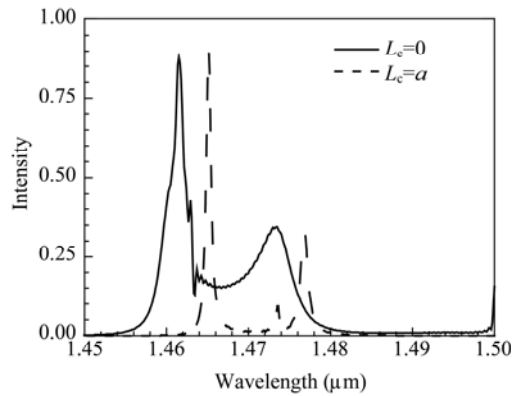
**Fig.4** Intensity spectra of TE polarization at port *D* for PCRR with traditional hexagonal-lattice inner ring with different  $L$  and  $L_c$



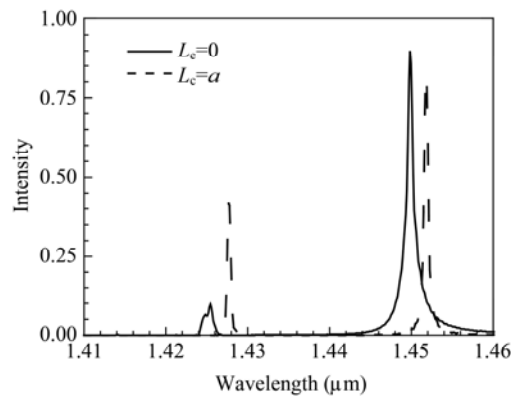
(a)  $L=3a$



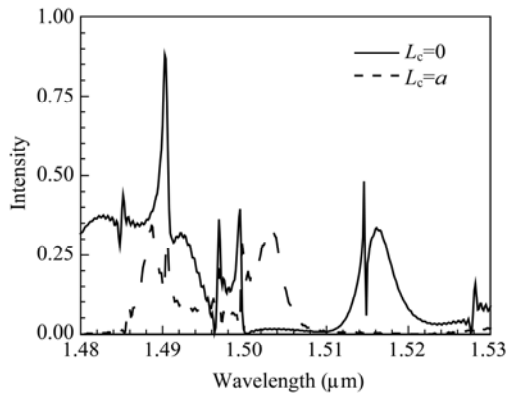
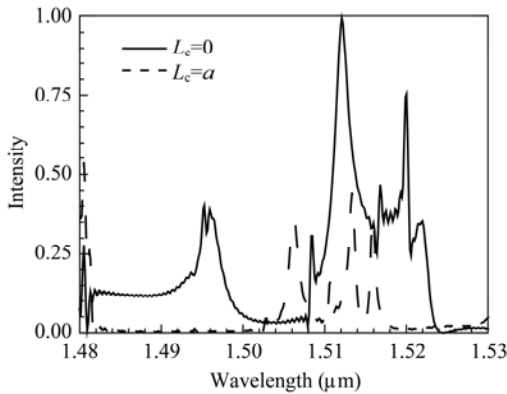
(b)  $L=4a$



(a)  $L=3a, R_c=1.5a$



(b)  $L=4a, R_c=2.3a$

(c)  $L=5a, R_c=2.8a$ (d)  $L=6a, R_c=3.2a$ 

**Fig.5 Intensity spectra of TE polarization at port D for PCRR with a large circular-hole inner ring with different  $L$  and  $L_c$**

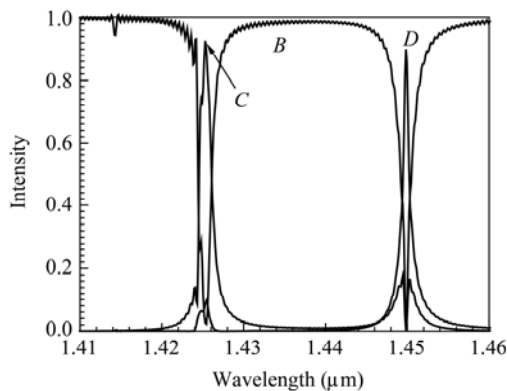


**Fig.6 Intensity spectra of TE polarization at three output ports B, C and D for our proposed large circular-hole inner ring, where  $L=4a$  and  $L_c=0$**

In conclusion, a new high-drop hexagonal-lattice silicon PCRR-based OADF is successfully demonstrated with width of bus waveguide as  $0.8\sqrt{3}a$ , side length of inner ring as  $4a$  and coupling strength as 0. Two channel wavelengths can be simultaneously dropped at two different output ports. For port D, the dropped channel is  $1.45\ \mu\text{m}$  with drop efficiency of 90.2% and quality factor of 1500, while for port C, the dropped channel is  $1.425\ \mu\text{m}$  with drop efficiency of 92.7% and quality factor of 950. Both traditional hexagonal-lattice inner ring and proposed configuration are sensitive to the changes of  $L$  and  $L_c$ . This makes the PCRRs become an alternative to current micro-ring resonators for ultra-compact WDM components and high density photonic integration.

## References

- [1] L. J. Zhou and A. W. Poon, *Optics Letters* **32**, 781 (2007).
- [2] S. Yuan, T. S. Wang and X. F. Liao, *Journal of Optoelectronics-Laser* **24**, 874 (2013). (in Chinese)
- [3] C. Li, L. J. Zhou and A. W. Poon, *Optics Express* **8**, 5069 (2007).
- [4] Z. X. Qiang, W. D. Zhou and R. A. Soref, *Optics Express* **15**, 1823 (2007).
- [5] Z. X. Qiang, R. A. Soref and W. D. Zhou, *Journal of Nanoscience Nanotechnology* **10**, 1495 (2010).
- [6] X. D. Lu, T. Zhou and S. X. Lun, *Journal of Optoelectronics-Laser* **23**, 83 (2012). (in Chinese)
- [7] M. Djavid, A. Ghaffari and M. S. Abrishamian, *Journal of the Optical Society of America B* **25**, 1829 (2008).
- [8] M. Djavid, B. S. Darki and M. S. Abrishamian, *Optics Communications* **284**, 1424 (2011).
- [9] X. F. Xu, H. X. Long and J. Z. Jiang, *Acta Photonica Sinica* **41**, 984 (2012).
- [10] X. Y. Ren, L. H. Feng and J. B. Feng, *Optics Letters* **38**, 1416 (2013).
- [11] M. Zetao and K. Ogusu, *Optics Communications* **284**, 1192 (2011).
- [12] S. H. Jeong, N. Yamamoto and J. I. Sugisaka, *Journal of the Optical Society of America B* **24**, 1951 (2007).
- [13] Tianbao Yu, Jiehui Huang, Nianhua Liu, Jianyi Yang, Qinghua Liao and Xiaoqing Jiang, *Applied Optics* **49**, 2168 (2010).
- [14] M. Qiu, *Applied Physics Letters* **81**, 1163 (2002).
- [15] Z. X. Qiang and W. D. Zhou, *IEEE Photonics Technology Letters* **18**, 1940 (2006).